

2D Ferromagnetism in the High- T_c Analogue Cs_2AgF_4

S.E.McLain,^{1,2} D.A.Tennant,^{3,4} J.F.C.Turner,² T.Barnes,^{5,6} M.R.Dolgos,² Th.Proffen⁷, B.C.Sales⁸ and R.I.Bewley¹

¹ISIS Facility, Rutherford Appleton Laboratory, Chilton, Didcot OX11 0QX, UK

²Department of Chemistry and Neutron Sciences Consortium,
University of Tennessee, Knoxville, TN 37996, USA

³Hahn-Meitner Institut, Glienicker Str. 18, Berlin D-14607,

Germany ⁴School of Physics and Astronomy, University of St.Andrews, St.Andrews, Fife KY16 9SS, UK

⁵Department of Physics and Astronomy and Neutron Sciences Consortium,
University of Tennessee, Knoxville, Tennessee 37996, USA

⁶Physics Division, Oak Ridge National Laboratory, Oak Ridge, TN 37831, USA

⁷LANSCe, Los Alamos National Laboratory, Los Alamos, NM 87545, USA

⁸Condensed Matter Sciences Division, Oak Ridge National Laboratory, Oak Ridge, TN 37831, USA

(Dated: June 19, 2018)

Although the precise mechanism of high- T_c superconductivity in the layered cuprates remains unknown, it is generally thought that strong 2D Heisenberg antiferromagnetism combined with disruptive hole doping is an essential aspect of the phenomenon. Intensive studies of other layered 3d transition metal systems have greatly extended our understanding of strongly correlated electron states, but to date have failed to show strong 2D antiferromagnetism or high- T_c superconductivity. For this reason the largely unexplored $4d^9$ Ag^{II} fluorides, which are structurally and perhaps magnetically similar to the $3d^9$ Cu^{II} cuprates, merit close study. Here we present a comprehensive study of magnetism in the layered Ag^{II} fluoride Cs_2AgF_4 , using magnetic susceptometry, neutron diffraction and inelastic neutron scattering techniques. We find that this material is well described as a 2D Heisenberg ferromagnet, in sharp contrast to the high- T_c cuprates. The exchange constant J is the largest known for any material of this type. We suggest that orbital ordering may be the origin of the ferromagnetism we observe in this material.

PACS numbers: 75.10.Jm, 75.25.+z, 75.30.Ds, 75.40.Gb

High- T_c cuprates are distinctive in having $[\text{CuO}_2]$ planes with very strong antiferromagnetic interactions between the spin-1/2 $3d^9$ Cu^{II} ions. Searches for antiferromagnetism with similarly large interactions in magnetic insulators containing other 3d spin-1/2 transition metal ions have not been successful to date. It may be instructive to extend the studies of magnetism in high- T_c analogues in another direction, to materials possessing spin-1/2 4d electrons. The spin-1/2 $4d^9$ Ag^{II} ion is an obvious first choice for this research program, as it is the heavier congener of Cu^{II} . Cuprates also show charge-transfer character, and it is known that doped holes preferentially reside on the oxygen sites in the $[\text{CuO}_2]$ planes rather than forming Cu^{III} ions. In silver fluorides analogous charge-transfer is anticipated for fluorine sites in $[\text{AgF}_2]$ planes [1].

Despite having common formal oxidation states, Cu and Ag show marked differences in oxidation-state stability: although Cu^{I} , Cu^{II} and Cu^{III} are all well represented in Cu chemistry, Ag^{I} and Ag^{III} dominate the solid-state and coordination chemistry of Ag [2, 3, 4]. To our knowledge, no oxide phases with $[\text{Ag}^{\text{II}}\text{O}_2]$ planes that are analogous to the cuprates exist, and AgO itself is best formulated as $[\text{Ag}^{\text{I}}\text{Ag}^{\text{III}}\text{O}_2]$ [2]. Ag^{II} is an unusual oxidation state for Ag, although materials containing this ion in a fluoride lattice are known.

Ag^{II} is a powerful oxidizer, which presents practical difficulties and requires the use of reagents and solvents such as F_2 or HF . However, using appropriate synthetic tech-

niques, compounds containing $\text{Ag}^{\text{II}}\text{F}_2$ square lattices can be prepared. In particular, ternary fluorides including Cs_2AgF_4 and Rb_2AgF_4 are known [5]. These compounds appear especially interesting as high- T_c analogues, since they are structurally very similar to K_2NiF_4 and are related to the high- T_c precursor La_2CuO_4 ; both families contain planes of $[\text{AgF}_2]$ or $[\text{CuO}_2]$ separated by planes of Cs/RbF or LaO. Few studies of these Ag^{II} compounds have been reported to date, and their magnetic properties are not well understood [1, 5]. Here we report detailed measurements of the magnetic properties of Cs_2AgF_4 , and compare with results for related materials.

The inverse of the measured molar static magnetic susceptibility of polycrystalline Cs_2AgF_4 (Methods) is shown in Figure 1. Our results are consistent with and extend the earlier data of Odenthal *et al.* [5]. Note that the qualitative behaviour is characteristic of a ferromagnet rather than an antiferromagnet such as La_2CuO_4 .

The structural and electronic similarity to La_2CuO_4 had suggested modelling magnetism in Cs_2AgF_4 with the 2D square lattice spin-1/2 Heisenberg antiferromagnet (HSqL), described by the Hamiltonian

$$H = J \sum_{\langle ij \rangle} \vec{S}_i \cdot \vec{S}_j \quad (1)$$

where $J > 0$ is the exchange constant. We find that this model actually does describe the susceptibility of Cs_2AgF_4 rather well over a wide range of temperatures, *albeit* with a ferromagnetic exchange constant ($J < 0$).

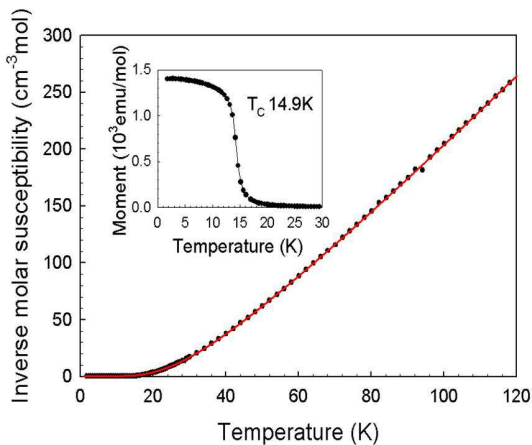


FIG. 1: Figure 1: The inverse of our measured molar susceptibility of Cs_2AgF_4 (points) after background subtraction. A fit to the theoretical susceptibility of the 2D spin-1/2 Heisenberg ferromagnet (the 10th order series of Baker *et al.* [6]) is shown as a solid line, and gives $g = 1.832$ and $J = -3.793$ meV. The insert shows the 15 K Curie transition and the low-temperature magnetic moment (with a simple interpolating curve).

Our fit to the susceptibility is shown in Figure 1; this gave the parameters $g = 1.832$ and $J = -3.793$ meV. We also considered 1D and 3D Heisenberg models, but these were found to be in clear disagreement with the measured susceptibility.

The Ag^{II} ion moment was estimated from a field-magnetization scan to be $0.8 \mu_B$ at 5 K, corresponding to $g = 1.6$; a value of $1.0 \mu_B$ would be expected for an isolated, isotropic spin-1/2 ion. Note that in a magnetization measurement the extracted ionic moment would be lowered by the presence of non-magnetic impurity phases. Covalency effects may also have lowered the moment in the pure material.

The predominant difference between Ag^{II} and Cu^{II} is the increase in the principle quantum number of the valence orbitals. In this ternary silver fluoride, the combination of lower Coulomb repulsion of $4d^9$ compared to $3d^9$ electrons and charge transfer properties anticipated for $\text{Ag}^{\text{II}}\text{F}_2$, which should differ from those of $\text{Cu}^{\text{II}}\text{F}_2$, may lead to new effects due to orbital fluctuations. The reduced g -value may be evidence for fluctuation or hybridization phenomena.

A ferromagnetic ordering (Curie) transition was observed in Cs_2AgF_4 near 15 K (see Figure 1 insert). Since an ideal 2D Heisenberg magnet only undergoes ordering at absolute zero [7], this 15 K transition signifies the presence of additional interactions such as anisotropies or interlayer coupling.

Although the bulk susceptibility is useful for characterizing the general magnetic behaviour of a material, establishing the nature of these interactions at the atomic

scale requires a local probe. Inelastic neutron scattering is ideal for this purpose, as the magnetic interaction strengths and pathways can be inferred from the energy and momentum transfer to the sample. As the impurities in the sample have very different magnetic properties than Cs_2AgF_4 , it is reasonable to assume that they will not interfere with the interpretation of the inelastic neutron scattering signal.

Figure 2 shows the results of our inelastic neutron scattering measurements. Figure 2(a) shows the scattering from Cs_2AgF_4 over the wavevector range $Q = 0.2 - 1.2 \text{ \AA}^{-1}$ at $T = 8$ K after background subtraction. Production of magnetic excitations is clearly observed above 6 meV. The magnetic nature of these excitations was confirmed by a decrease in intensity and broadening of the signal upon heating to 35 K. For comparison, Figure 2(b) shows the scattering predicted by the ferromagnetic 2D spin-1/2 Heisenberg model with $J = -5.0$ meV.

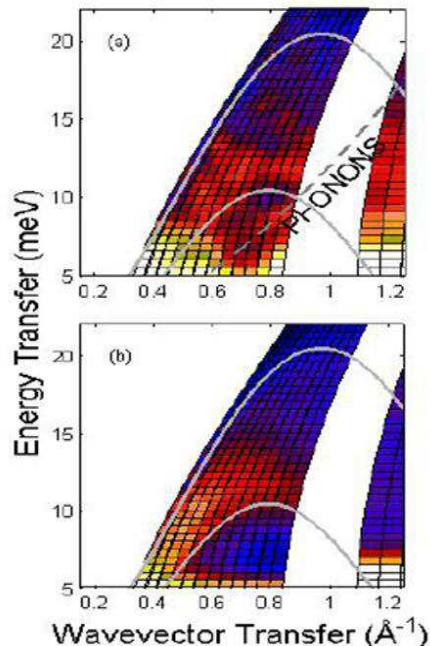


FIG. 2: Figure 2: (a) Low-wavevector inelastic neutron scattering from Cs_2AgF_4 at 8 K, using $E_i = 100$ meV, corrected as described in text. The intensity of scattering is indicated by the colour scale. Below an energy transfer of 6 meV, incoherent scattering processes are dominant. Magnetic excitations are observed from $0.4 - 1 \text{ \AA}^{-1}$ and 6 - 15 meV. Solid grey lines bound the region in which appreciable scattering from magnetic excitations is expected. The grey dashed curve indicates the onset of significant phonon scattering relative to the weak ferromagnetic scattering (above $\sim 1 \text{ \AA}^{-1}$). (b) Simulated scattering for a 2D spin-1/2 Heisenberg ferromagnet, using an exchange constant of $J = -5.0$ meV.

To determine J , scans in energy at constant wavevector were extracted and the peak positions were determined

by fitting Gaussian profiles to these data. The data and fits are shown in Figure 3 (main panel). The dispersion relation for ferromagnons in the 2D Heisenberg model was fitted to this data after correcting for instrumental effects, yielding $J = -5.0(4)$ meV for the exchange constant in Cs_2AgF_4 . (Recall that the fit to the susceptibility gave a somewhat lower value of $J = -3.8$ meV.) For wavevectors above $\sim 1\text{\AA}^{-1}$, scattering from phonons becomes dominant, so the higher- Q data was not fitted. Below 6 meV, quasi-elastic incoherent scattering masks any magnetic signal that may be present.

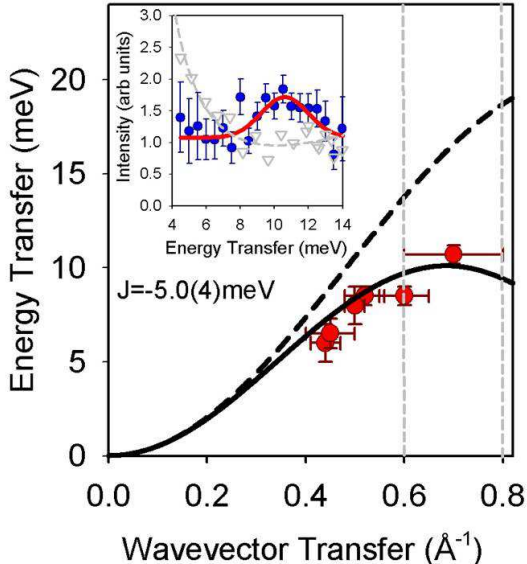


FIG. 3: Figure 3: (inset) Inelastic neutron scattering from Cs_2AgF_4 with $E_i = 50$ meV, at temperatures of 8 K (blue circles) and 35 K (grey triangles), showing the range $0.6 - 0.8 \text{\AA}^{-1}$. The line through the data is a fit as described in the text. (main panel) Fitted positions of scattering in wavevector and energy are plotted, corrected for resolution. Dynamical scattering for the ferromagnetic powder lies in a continuum of values bounded by the lower solid and upper dashed curves.

The ferromagnetism we observe in Cs_2AgF_4 is in striking contrast to the antiferromagnetism in La_2CuO_4 , and is instead reminiscent of K_2CuF_4 . This material is one of the few known 2D spin-1/2 ferromagnetic insulators [8, 9], and like Cs_2AgF_4 is a Heisenberg ferromagnet, with $J = -1.0$ meV and $T_{\text{Curie}} = 6.25$ K [9]. The ferromagnetism in K_2CuF_4 has been attributed to a cooperative Jahn-Teller distortion and associated orbital ordering [10, 11], as depicted in Figure 4(c).

According to the Jahn-Teller theorem [12], the stereochemistry of a d^9 metal ion should distort so as to lower both the symmetry and the energy of the system. For a hypothetical $\text{Ag}^{\text{II}}\text{F}_6$ octahedron, in which the Ag^{II} ion is in a $t_{2g}^6 e_g^3$ electronic state, two structural pathways are commonly observed for this distortion [13]. Axial compression of the octahedron results in a partially filled a_{1g}

($\sim 3z^2 - r^2$) ground state orbital, whereas axial elongation results in a b_{1g} ($\sim x^2 - y^2$) ground state [13, 14]. Both distortions give rise to the same D_{4h} local point group, which is the local symmetry of the Ag^{II} ion in the space group $I4/mmm$.

There is, however, no known example of a system in which the electronic ground state is a_{1g} ($\sim 3z^2 - r^2$) [15]; rather, systems that show axial compression are better described using a partially filled ($z^2 - x^2$) and ($z^2 - y^2$) basis on the metal center [11, 14]. The magnitude and precise nature of the distortion will depend, *inter alia*, on the axial electrostatic potential and anisotropic elastic constants for axial *versus* equatorial ligand displacement [16], but the orbital occupancies and symmetries themselves will conform to this general model. In the square lattice copper halides K_2CuF_4 [9] and $(\text{C}_2\text{H}_5\text{NH}_3)_2\text{CuCl}_4$ [17], a_{1g} and b_{1g} orbital states couple to each other and to the electron spin and lattice degrees of freedom, producing a complex nonlinear Hamiltonian that involves all these degrees of freedom [18]. An antiferrodistortive pattern of ($\sim z^2 - x^2$) and ($\sim z^2 - y^2$) hole orbitals results, giving a strong ferromagnetic state. In this state, the fluorine atoms are displaced from their symmetric $I4/mmm$ positions, lowering the symmetry to $Bbcm$. We suggest that a similar mechanism is responsible for the observed ferromagnetism in Cs_2AgF_4 . If the difference in the exchange constant J measured above and below T_c is significant (-5 meV from neutron scattering versus -3.8 meV from the susceptibility), it may be associated with this orbital ordering transition.

Orbital ordering has been observed in other systems; cooperative orbital order in pseudo-cubic KCuF_3 leads to strong 1D antiferromagnetism, and strong antiferromagnetism has also been reported in KAgF_3 , in which evidence for conduction above 50 K has been reported [19]. However the absence of strong 2D antiferromagnetism among the copper halides in general suggests that the arrangement of pseudo-octahedra in the perovskites or associated Ruddlesden-Popper phases is important.

In a search for evidence of this structural distortion in Cs_2AgF_4 , we carried out neutron diffraction measurements on Cs_2AgF_4 at 6 K and 298 K. The data were fit using the Rietveld method assuming the space groups $I4/mmm$ and $Bbcm$, the latter being the space group of the orbitally ordered phase of K_2CuF_4 [10]. As no significant difference in the quality of fit was observed between the $I4/mmm$ - and $Bbcm$ -symmetry models, our results are consistent with either space group. However, we note that the atomic displacement parameters for the equatorial fluorine atoms in the AgF_6 pseudo-octahedra are large, which may be a signature of disorder in the plane; the resolution of our diffraction experiments does not allow discrimination of this disorder. This may be due to the limitation of statistics for a highly absorbing sample, in which small shifts in position may not be easily detectable. These diffraction measurements showed that

the AgF_6 pseudo-octahedra in Cs_2AgF_4 are compressed, which is inconsistent with the b_{1g} ground state familiar in La_2CuO_4 ; in that case the CuO_6 pseudo-octahedra show axial extension (see Figure 4(a)). Future investigations are planned, using high resolution neutron diffraction and resonant X-ray diffraction [20, 21], which should clarify the precise nature of the orbital ordering.

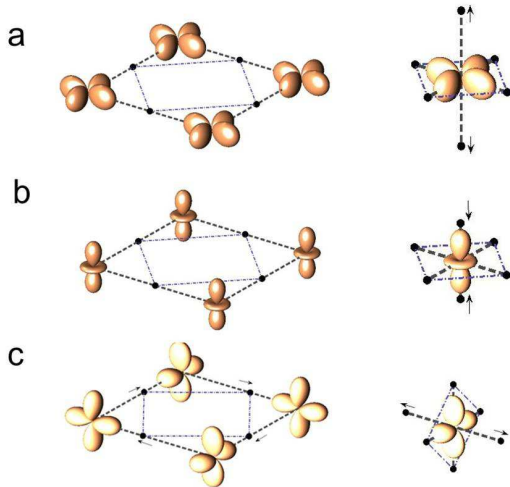


FIG. 4: Figure 4: Orbital ordering scenarios for Jahn-Teller active $3d^9$ and $4d^9$ layered perovskites. (a) Formation of a b_{1g} ground state with partially filled $\sim x^2 - y^2$ orbitals is accompanied by axial extension of octahedral ligands (right). Large in-plane overlap with ligand p -orbitals gives very strong antiferromagnetism, as is found in the high- T_c cuprates. (b) Formation of a_{1g} ground states (partial filled $\sim 3z^2 - r^2$ orbitals) is accompanied by axial compression (right). Weak 2D ferromagnetism in the layers or 1D behaviour between layers may occur. (c) Anharmonic coupling to ligands favours the formation of staggered orbital ordering of $\sim z^2 - x^2$ and $\sim z^2 - y^2$ orbitals, as in K_2CuF_4 . In-plane ligands are displaced from central positions, lowering the crystal symmetry. Strong ferromagnetic superexchange occurs through the unfilled in-plane orbitals.

The different d -orbital orientations proposed for Cs_2AgF_4 and La_2CuO_4 may have a simple origin in the electrostatics of these materials. In the cuprates, the $[\text{CuO}_2]$ layers possess a net negative charge, having two electrons per formula unit. For this reason it is energetically favourable for the positively charged holes to lie in the ab plane, localized in b_{1g} orbitals. In contrast the $[\text{AgF}_2]$ layers in Cs_2AgF_4 are charge neutral, so there is no strong electrostatic orientation preference. (a_{1g} states are expected to be slightly preferred [16].) To test the stability of the assumed a_{1g} configuration of Cs_2AgF_4 , we have also synthesized the isostructural Rb_2AgF_4 [5]. This material shows magnetic properties very similar to Cs_2AgF_4 , demonstrating that this magneto-orbital configuration is robust. We speculate that charge-doping of Ag^{II} fluorides may alter the electrostatic forces suffi-

ciently to allow in-plane holes and stabilize a strong antiferromagnetic state. Our initial investigation of electron-doped $\text{Cs}_{2-x}\text{Ba}_x\text{AgF}_4$ for $0 < x < 0.3$ however has not identified an antiferromagnetic state [22].

The structural similarity to the high- T_c precursor La_2CuO_4 , combined with our confirmation of strong magnetic interactions between the Ag^{II} ions in Cs_2AgF_4 , suggests the possibility of a rich variety of magnetic phases in Ag^{II} fluorides [1]. Given the oxidizing power of Ag^{II} , it is unlikely that other non-fluoride anion lattices will accommodate this species; accordingly, we are currently exploring ternary and quaternary Ag^{II} -fluoride Ruddlesden-Popper phases [22]. High pressure experiments, which have proved fruitful in other systems [17], may also be particularly interesting.

In summary, we have found that the layered silver fluoride Cs_2AgF_4 is well described magnetically as a 2D spin-1/2 Heisenberg ferromagnet, and the exchange constant J is the largest known for any magnetic material of this type. These conclusions followed from measurements of both static (susceptibility) and dynamic (inelastic neutron scattering) magnetic properties of polycrystalline Cs_2AgF_4 .

ACKNOWLEDGEMENTS

We would like to thank J. A. del Toro and the staff at the University of Liverpool for the use of their SQUID magnetometer, D. Scalapino, D. I. Khomskii and D. J. Singh for critical readings of the manuscript, and D. Argyriou and S.M. Bennington for useful discussions. S. E. McLain acknowledges support from the U.S. National Science Foundation through award OISE-0404938. Financial support was also provided by the EU through the Human Potential Programme under IHP-ARI contract HPRI-CT-1999-00020, the Manuel Lujan Neutron Scattering Center, funded by the U.S. Department of Energy Office of Basic Energy Sciences, and Los Alamos National Laboratory, funded by the U.S. Department of Energy under contract W-7405-ENG-36. J. F. C. Turner acknowledges the financial support of the U.S. National Science Foundation, through a CAREER award (Grant No. CHE 0349010), and the University of Tennessee through the Neutron Sciences Consortium.

METHODS

Cs_2AgF_4 was prepared through a solid state reaction between AgF_2 and CsF (Fluorochem USA). In a typical preparation, 0.0178 mol of AgF_2 and 0.0356 mol of CsF were ground together in a dry box in an inert atmosphere of argon or N_2 using an agate mortar and pestle until they formed a visually homogenous mixture. The mixture was then transferred to a pure gold reaction tube

(height 9 cm, i.d. 1.5 cm) and placed inside a Schlenk flask and subsequently heated to 270°C under a flow of argon for 24 hours. The resulting lilac coloured solid was stored in an N₂-filled glove box in a desiccator over NaK₃ alloy. Sample purity was checked by X-ray powder diffraction using a Bruker AXS Smart 1000 diffractometer equipped with a graphite monochromatized Mo-K α source. The observed pattern and positions of diffraction rings corresponded to the Cs₂AgF₄ unit cell parameters reported previously [5]. X-ray diffraction experiments at NSLS also confirmed the nature of the phases.

For the SQUID measurements, approximately 100 mg of Cs₂AgF₄ powder was loaded into prefluorinated PTFE sample holders under an argon atmosphere. Measurements were made using a Quantum Design SQUID magnetometer, under a weak applied field of 100 Oe. For the neutron diffraction measurements, approximately 0.5 g of Cs₂AgF₄ powder was loaded into flame-dried quartz tubing (o.d. 0.4 cm, i.d. 0.30 cm), also under an argon atmosphere and subsequently flame-sealed under vacuum (*ca.* 10⁻³ mbar). Measurements were performed using the Neutron Powder Diffractometer (NPDF) at the Manuel Lujan Neutron Scattering Center at Los Alamos National Laboratory. All diffraction data were corrected for background scattering, incident neutron flux, multiple scattering and absorption effects, using the PDFgetN analysis procedures [23]. The data were analysed using reciprocal space Rietveld refinements, performed with the GSAS package [24], and yielded the tetragonal lattice parameters $a = b = 4.5573(14)$ Å and $c = 14.166(6)$ Å at 6 K, and $a = b = 4.5905(18)$ Å and $c = 14.213(6)$ Å at 295 K, consistent with previous reports [5]. Multiphase Rietveld refinement of these data showed the presence of small quantities of AgF and CsF at the level of a few mole percent.

For the inelastic neutron scattering measurements, approximately 10 g of Cs₂AgF₄ powder were loaded into scattering cells under an argon atmosphere. As the neutron absorption cross-section for Ag is quite large (63.3 barns), a thin plate Al sample cell (3 mm width) was utilized. The sample was initially placed in an envelope of prefluorinated PTFE sheet (5 cm x 5 cm x 0.01 mm) to prevent a chemical reaction with the aluminium sample cell. Measurements were performed using the High Energy Transfer (HET) time-of-flight spectrometer at the ISIS pulsed neutron source, Rutherford Appleton Laboratory, UK. HET is a direct geometry chopper spectrometer with large angular ³He detector coverage, from scattering angles of $\phi = 3^\circ$ to 7° (4 m) and $\phi = 9^\circ$ to 29° (2.5 m) in two separate banks, which makes it especially effective for the study of neutron scattering from powders. Incident energies of 50 and 100 meV were selected and measurements made at temperatures of 8 K, 35 K and 295 K. Typical measurement times were

10 hours per run at an average proton current of 1700 μ A. Empty cell runs were also performed at the same energies and temperatures. All data were corrected individually for incident neutron flux and detector efficiencies. Empty cell runs were then corrected for sample absorption effects before being subtracted from the data sets obtained from the powder sample itself. This subtraction was necessary because scattering from PTFE remains significant at the low wave-vectors associated with magnetic excitations.

-
- [1] W.Grochala and R.Hoffmann, *Angew. Chem., Int. Ed. Engl.* 40, 2742 (2001).
 - [2] H.Muller-Buschbaum, *Z. Anorg. Allg. Chem.* 630, 2125 (2004).
 - [3] D.Srochinski, Y.Dziegiec and A.Grzejdziaak, *Russ. J. Coord. Chem.* 23, 447 (1997).
 - [4] C.E.Housecroft, *Coord. Chem. Reviews* 115, 141 (1992).
 - [5] R.-H.Odenthal, D.Paus und R.Hoppe, *Z. Anorg. Allg. Chem.* 407, 144 (1974).
 - [6] G.A.Baker, Jr., H.E.Gilbert, J.Eve and G.S.Rushbrooke, "On the Two-Dimensional, Spin-1/2 Heisenberg Ferromagnetic Models", *Phys. Lett.* A25, 207-209 (1967).
 - [7] N.D.Mermin and H.Wagner, *Phys. Rev. Lett.* 17, 1133 (1966).
 - [8] F.Moussa and J.Villain, *J. Phys. C9*, 4433 (1976).
 - [9] W-H.Li, C.H.Perry, J.B.Sokoloff, V.Wagner, M.E.Chen and G.Shirane, *Phys. Rev.* B35, 1891 (1987).
 - [10] M.Hidaka, K.Inoue, I.Yamada and P.J.Walker, *Physica B+C (Amsterdam)* 121, 343 (1983).
 - [11] D.I.Khomskii and K.I.Kugel, *Solid State Commun.* 13, 763 (1973).
 - [12] H.A.Jahn and E.Teller, *Proc. Roy. Soc. (London)* A161, 220 (1937).
 - [13] T.A.Albright, J.K.Burdett and M-H.Whangbo, *Orbital Interactions in Chemistry* (Wiley, New York, 1985).
 - [14] H.J.Koo and M-H.Whangbo, *J. Sol. State Chem.* 151, 96 (2000).
 - [15] D.I.Khomskii, private communication.
 - [16] J.M.Garcia-Lastra, J.A.Aramburu, M.T.Barriuso and M.Moreno, *Phys. Rev. Lett.* 93, 226402 (2004).
 - [17] Y.Moritomo and Y.Tokura, *J. Chem. Phys.* 101, 1763 (1994).
 - [18] M.V.Mostovoy and D.I.Khomskii, *Phys. Rev. Lett.* 92, 167201 (2004).
 - [19] W.Grochala and P.P.Edwards, *Phys. Stat. Sol. (B)* 240, R11-R14 (2003).
 - [20] H.Manaka, T.Koide, T.Shidara and I.Yamada, *Phys. Rev.* B68, 184412 (2003).
 - [21] N.Binggeli and M.Altarelli, *Phys. Rev.* B70, 085117 (2004).
 - [22] M.R.Dolgos *et al.* (unpublished).
 - [23] P.F.Peterson, M.Gutmann, T.Proffen and S.J.L.Billinge, *J. Appl. Cryst.* 33, 1192 (2000).
 - [24] A.C.Larson and R.B.vonDreele, Los Alamos report LAUR 86-748.